Research article Available online www.ijsrr.org ISSN: 2279–0543

International Journal of Scientific Research and Reviews

Analysis of Characterization, Magnetic and Anti-Bacterial Properties of Zinc Doped with Nano-Crystalline Cobalt Ferrite Prepared by Co-precipitation Method

S. Sobana[a], S. Alagumanian[b], P. Shakthivel[c] and P. Sivakumar[a*],

[a] PG and Research Department of Physics, Periyar E. V. R. College (Autonomous), Tiruchirappalli, Pin – 620023, TN, India. Email – sobana1283@gmail.com

[b] PG and Research Department of Botany, H.H.The Rajah's College (Autonomous), Pudukkottai, Pin – 622001, TN, India. Email – salagumanian@yahoo.co.in

c Department of Nanoscience and Technology, Alagappa University, Karaikudi – 630002, TN, India.

ABSTRACT

Nano-crystalline Zn doped cobalt ferrite powders (0.0, 0.2, 0.4, 0.6, 0.8 and 1.0) were effectively combined of "Green Chemistry" new material for acquiring nanoparticles by compound co-precipitation technique has been produced. The auxiliary, morphological and attractive properties of the items were controlled by X-ray diffraction (XRD), Scanning Electron Microscopy (SEM), Transmission Electron Microscopy (TEM) and Vibrating Sample Magnetometery (VSM). X-ray investigation demonstrated that the examples were cubic spinel. SEM pictures uncover that the examples' surfaces display very much characterized crystalline nanoparticles of circular shapes with little agglomeration. Raman spectra also prove spinel ferrite crystal structure of synthesized nanoparticles. The expansion of Zn particles caused a reduction in the normal crystallite size, polarization and the coercive field of the example. The watched reductions in immersion charge and coercivity are clarified on the bases of exchange interactions. The nearness of superparamagnetism with little coercivity (delicate ferrite) demonstrating the examples are great possibility for applications in high-recurrence transformers.

KEY WORDS; Zn, Magnetic nanoparticles, TEM, XRD and FTIR

[*]Corresponding Author

P. Sivakumar

PG and Research Department of Physics,

Periyar E. V. R. College (Autonomous),

Tiruchirappalli, Pin – 620023, TN, India.

E. Mail; sivakumarpsk72@gmail.com

INTRODUCTION

Investigators have been concerned in studying materials in their nanoscale dimensions due to their high surface area resulting to developed properties in comparison with the bulk materials counterpart[1–6]. Spinel ferrite (SF) materials with a common formula of AFe_2O_4, where A stands for metals as (Mn, Co, Ni, Mg, or Zn), are well known of their remarkable electrical, optical, and magnetic properties, especially in nanometer scale [7–9]. Doping with metal ions as (Zn, Co, Sr, and Gd) was aimed to developed the physicochemical properties of ferrite nanoparticles (NPs) essential for their use such as photocatalysis [10, 11] in photo degradation of dyes and as antibacterial agents [12, 13], industrial applications [14], and electrochemical energy storage materials[15, 16]. Studies proved that doping influences the structural [17], optical [18], electrical [17, 19], infrared radiation properties [20, 21], and magnetic properties [22, 23]

Cobalt ferrite is a ferromagnetic cubic spinel and important in numerous scientific uses such as magnetic recording media, magnetic refrigerators, microwave devices and other high frequency appliances [24]. It is a well-known hard ferrite material that has been studied in detail, due to its very high cubic magneto crystalline anisotropy, reasonably saturated magnetization, high wear resistance and good electrical insulation [25]. It displays different magnetic properties depending on the thermal history, composition and site preference of the cations among the tetrahedral (A) and octahedral (B) sites [24-26]. The partial substitution of transition metal in the $CoFe_2O_4$ offers an excellent chance for engineering specific magnetic interactions in the crystal lattice [27]. The addition of nonmagnetic zinc in cobalt ferrite raises saturated magnetization, due to zinc being the transition metal with strong A-site preference [26]. Thus, Y. K¨oseo˘gul *et al*. [25] prepared a cobalt zinc ferrite nano particle by using the microwave method. It was recorded from the magnetic properties studied that the composition, $Co0.8Zn0.2Fe_2O_4$, has the highest value of saturated magnetization. However, the oxidative state of all elements in the samples has still to be examined in any great extent. Therefore, this work aimed to study the valence state of structural elements by synthesizing $CoFe_2$-$xZnxO_4$ powders using solid state reaction, which is a very easy and the significant economical method [28]. The samples were characterized by various techniques and then studied for their structure, magnetic behavior and oxidative state of each structural element.

It is well known that the preparation technique has a direct influence on the nanoparticle's shape and size and thus can affect the physical and chemical properties of nanostructures. The magnetic ferrite particles in the nanoscale regime can be synthesized by different method like soft chemical techniques such as co-precipitation, hydrothermal, sol–gel, etc. But the major benefit of co precipitation technique resides in offering particle size in the nanoscale regime with a high crystallinity. Such individual nanoparticles have a large constant magnetic moment and performed

like a giant paramagnetic atom with a rapid response to applied magnetic field with negligible remanence and coercivity (super magnetic behavior). Nanoparticles can also result in a low saturation magnetization. These features make super paramagnetic nanoparticles very attractive for a broad range of application in particular biomedical field. Therefore, the magnetic properties of nanoparticles highly depend upon the synthesis technique. Nanocrystalline $CoFe_2O_4$ with unique properties has potential uses in high frequency device, memory core, recording media, and in biomedical field. It is known that zinc ions (Zn^{2+}) with diamagnetic nature are recognized for achieving good control over magnetic parameters in increasing technically important materials. Substitution of magnetic (Co^{2+}) by a nonmagnetic (Zn^{2+}) cations in spinel ferrite phase may induce significant alteration in their structural, optical, magnetic, and others properties, due to the distribution of cations in between the available A and B sites. However, a detailed study on the structural, elastic, optical, and magnetic properties of Zn^{2+}-doped $CoFe_2O_4$ nanoparticles obtained by co-precipitation technique in the largely region has not still been recorded so far. The aim of the new work is to synthesize nanoparticles of $Co1-xZnxFe_2O_4$ with x differing from 0 to 1% from metal salts by co-precipitation of hydroxides. The influence of Zn substitution on the structural, optical, and magnetic properties for this system has also been discussed.

MATERIALS AND METHODS

Materials

The forerunners Co $(NO_3)_2$•$6H_2O$, (Merck, Kenilworth, NJ, USA) and Fe $(NO_3)_3$•$9H_2O$ (Merck) were used as oxidizing specialists. The two synthetic concoctions were of explanatory review and used without more refinement. *Eichhornia crassipes* plant extract was used as the reducing agent. Each alignment was prepared utilized deionized water.

Preparation of Plant Extract

Eichhornia crassipes is one of the helpful curative plants which got from the South America. *Eichhornia crassipes* is known as Water Hyacinth in common name and also known as Venkayattamarai and Jalakumbi; *Eichhornia crassipes* extricate was prepared utilized 5 g segments of products, which were totally washed without the use of dangerous natural mixes. The supernatant was expelled, and the internal part (gel of the plant) was finely cut and mix together with 30 ml of deionized water. This blend was modified for 1 h used an attractive stirrer at 32°C to frame a homogeneous alignment. The arrangement was sifted and used as the concentrate.

Preparation of Tin-Substituted Cobalt Nano-Ferrites

A progression of Sn doped cobalt ferrite test were prepared with the nonexclusive equation $CoZn_x\ Fe_{2-x}O_4$ (0.0, 0.2, 0.4, 0.6, 0.8 and1.0) due to standard synthetic co-precipitation strategy. Stoichiometric measure of explanatory review Co $(NO_3)_2 .6H_2O$, Sn $(NO_3)_2 .9H_2O$, $FeCl_3$, were broken up in de-ionized water and blended on an attractive plate. The concentrate of *Alfalfa* was then added drop to the solution beneath overwhelming blending for a few hours at room temperature till the point when a reasonable alignment was acquired. To the above alignment, NaOH was slowly having drop shrewd till the pH of the arrangement turned 7. The pH of the arrangement was raised to 10 and from that point, procedure for two hours at 80ºC with persistent blending to guarantee significant response occurred. The arrangement was cooled and rinsed with de-ionized water over and over to convey the pH down to 7. Subsequent to evacuating the abundance hydroxyl particles, the arrangement was at long last washed with ethanol, and left to dry. The dried examples were sintered at 1100°C for 3 hours and ground to get a mass of fine dark powder. Every one of the portrayals was acted with this dark powder. The auxiliary portrayal of the example was complete using a Rigaku: Ultima IV X-beam diffractometer with a Cu goal containing trademark wavelength Cu-Kα of 1.5406 Aº. The example was at a rate of 0.02° each second in the precise scope of 20° to 80°. The transmission electron microscopy was totally used a JEOL 2010 model electron magnifying lens. The hysteresis and the M-T estimations were totally used a SQUID magnetometer (Quantum Design). The examples are assigned as Zn0.0, Zn 0.2, Zn 0.4, Zn 0.6, Zn 0.8 and Zn 1.0 as per the grouping of dopant (Zn) recent in the example.

Characterization Techniques

Auxiliary distinguishing proof and stage research of Zn-Co ferrites were totally by XRD thinks about using Bruker D8 advance (Model No. 204795) X- ray beam Diffractometer. The XRD estimations were acted by CuKα radiation (λ = 1.5406 Å) in the scope of 2θ = 20° to 80° in the means of 0.02°. Spinel sorts of valuable stone structure without containing a few further middle of the road stages and high virtue stage of constituent powders were affirmed by XRD think about. The Fourier Transform Infrared (FTIR) spectra of the got powders were recorded used FTIR spectrometer (Thermo electron organization, Serial No: AEU0500303) in the wave number range 4000 cm−1 to 500 cm−1 using Br pellets to endorse the spinel structure of the examples. Transmission Electron Microscope (TEM) strategy was used with the final objective to research the nanostructure of the item material. The example for TEM was prepared by setting a drop of ethanol suspension of the nanoparticles on carbon-covered Cu TEM frameworks. The networks were examined using a transmission electron magnifying lens (FEI Tecnai G2 S-Twin 200 kV). With the

last aim to think about the attractive properties, VSM (Lake Shore display 7407) examination was utilized at a room temperature with greatest connected attractive field of 15 kG.

Bacterial Strains and Cultivation

Bacterial strains including *Escherichia coli, S. Haemolyticus, Aeromonas hydrophila, Cronobacter sakazakii, Aeromonas salmonicida* and *Basillus subtilis* were used for experiment. 50ml of LB broth was prepared in 250ml conical flask and the bacterial strains were grown in this medium at $37^{0.}$C on an orbital shaker. The culture flask was inoculated at 0.1 OD 600nm with freshly prepared LB medium under same culture conditions. The mid log phase bacterial cultures were used for the antibacterial studies.

Disk Diffusion Method

0.1 OD of overnight different bacterial cultures was swabbed on the 25ml LB agar plates. Then the whatman disk was placed on the plates. About 30ul of of undoped and Zn doped samples were add on that whatman disc and incubate for overnight at 37^{o}C. Streptomycin was used as a standard.

RESULTS AND DISCUSSION

X-ray Diffraction Analysis

X-ray diffraction (XRD) was performed on the powders calcined at 800 °C and the XRD patterns of every the samples were shown in Fig. 1. The obtained patterns confirmed the formation of a homogeneous single phase having cubic spinel structure with the space group Fd3m. The patterns showed diffraction peaks of $Co_{1-x}Zn_xFe_2O_4$ (x = 0.0, 02, 0.4, 0.6, 0.8, 1), corresponding to (220), (311), (400), (331), and (440) reflections. All XRD patterns are investigated by utilizing the Rietveld technique and FullProf program. The result shows that the lattice parameter a slightly increases with Zn^{2+}-doping content as shown in Table 1. The increase of a with x can be explained on the basis of the difference in ionic radii of Zn^{2+} and $Co^{2+.}$ The smaller ionic radius of Co (0.58 Å) was replaced by the larger ionic radius of Zn (0.6 Å) so the lattice parameter increased due to the enlargement of the unit cell. By dividing Kα-doublet of every observed peak, it is found that the peaks would be implicitly described by the Cauchy function. Therefore, while determining the physical broadening, the hardware broadening is subtracted from the integral width of the experimental peaks. Considering that, the forms of mathematical functions that described different type of physical broadening are unknown, thereby different method were roposed to determine microstructural parameters (crystallite size and microstrain). The analysis of the crystallite size has been carried out

using the broadening of XRD peaks. It is known that peak broadening results from both finite crystallite size and strain effect within the crystal lattice [29].

The broad XRD lines in the pattern indicate that the particles are in nano scale. From the XRD data crystallite size was calculated using Scherrer's formula Eq [30].

$$D = \frac{k\lambda}{\beta cos\theta} \qquad (1)$$

Where λ is the wavelength of the X-ray used (1.5406 Å), β is the full width at half maximum.

The lattice constant (a), hoping length for tetra (La) and octahedral (Lb) sites were obtained from the following relations [31].

$$a = d(h^2 + k^2 + l^2)^{\frac{1}{2}} \qquad (2)$$

$$L_a = 0.25a\sqrt{3} \qquad (3)$$

$$L_b = 0.25a\sqrt{2} \qquad (4)$$

Where 'd' is spacing between the planes, (h,k,l) are the miller indices. The calculated lattice constant (a), particle size (D), tetrahedral and octahedral hoping length are tabulated in Table 1. From the Table 1, it is evident that the decrease in the value of lattice constant, crystallite size and tetrahedral and octahedral hoping length with increase in Cr content. The decrease in lattice constant takes place due to the difference between the ionic sizes of Fe^{3+} (0.645 A°) and the substituted Zn (0.615 Aº) ions. It is well known that the Hoping length explains the distance between the magnetic ions and provides valuable information about strength of spin interaction. The difference in ionic radius between the impurity cations and the substituted cations are the strong indications for change in hoping length [32].

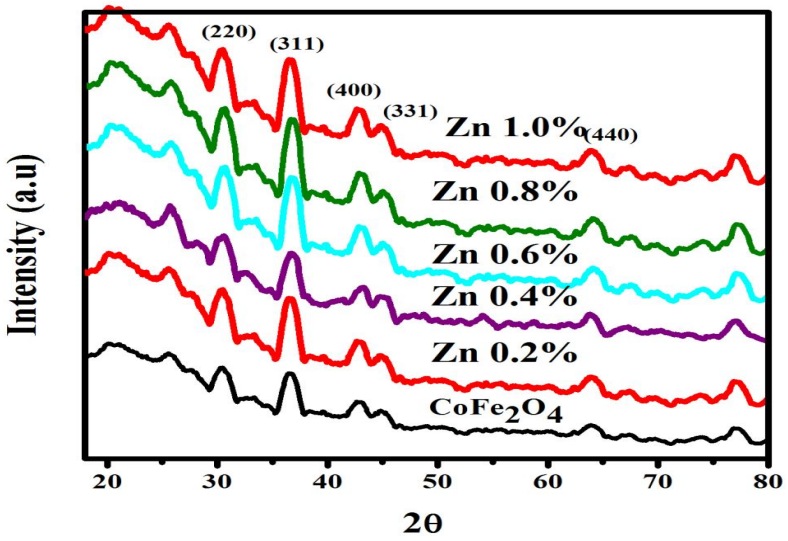

Fig.1- X-ray diffraction pattern of (a) pure, (b) 0.2%, (c) 0.4%, (d) 0.6%, (e) 0.8% and (f) 1.0 % Zn doped Co-ferrite samples

Table 1- Structural parameters of $Zn_xCoFe_{2-x}O_4$ (x = 0.0 to 1.0).

Compound (x) (Zn)	Lattice constant (a) (A°)	Average Particle size (D) nm	L_a (A°)	L_b (A°)
0	8.3945	38	3.6384	2.9668
0.2	8.3917	31	3.6335	2.9659
0.4	8.3880	30	3.6314	2.9646
0.6	8.3860	26	3.6303	2.9638
0.8	8.3824	24	3.6285	2.9626
1	8.3806	21	3.6276	2.9619

Surface Morphology of Co-Zn Ferrites

The scanning electron micrographs (SEM) of Zn-doped $CoFe_2O_4$ models (with x = 0.2 and x = 1) shown in Fig. 2 displayed the formation of agglomerates of very fine particles with almost spherical shape. It can be seen that the Fig. 2 showed heavily concentrated particles of nanoscale regime for Co0.8Zn0.2Fe_2O_4 and Co0.5Zn1Fe2O4 samples. This is due to its permanent magnetic moment; hence, each particle is permanently magnetized and tends to agglomerate with other particles. The Zn substituted nanoparticles possess higher magnetic moment leading to more clustering.

All the SEM pictures have homogeneous grain estimate circulation, very much pressed and are relatively break free. Agglomeration of nanoparticles occur because of the presence of these agglomerates might sinter process as of concoction response. It is accounted for that if there should happen an occurrence of a spinel ferrite, the molecule estimate diminishes because of a solid site inclination of doping component. This process prompts restrict the nucleation procedure and size amid the molecule development. In the recent examination 1.0% Zn doped example (Fig. 2) displayed homogeneous and better nanoparticles which are further responsive and consequently more agglomerated contrasted with undoped test.

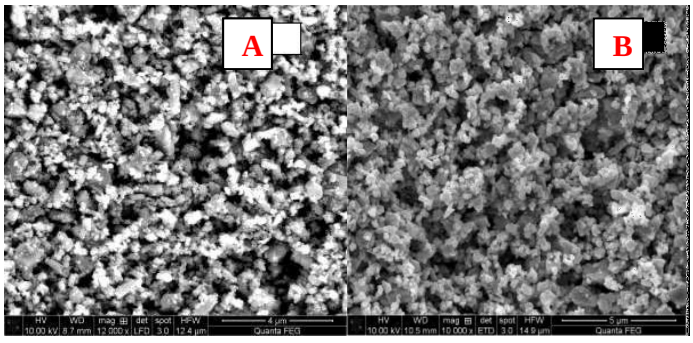

Fig. 2- SEM images of (a) undoped and (b) 1.0 % Zn doped samples.

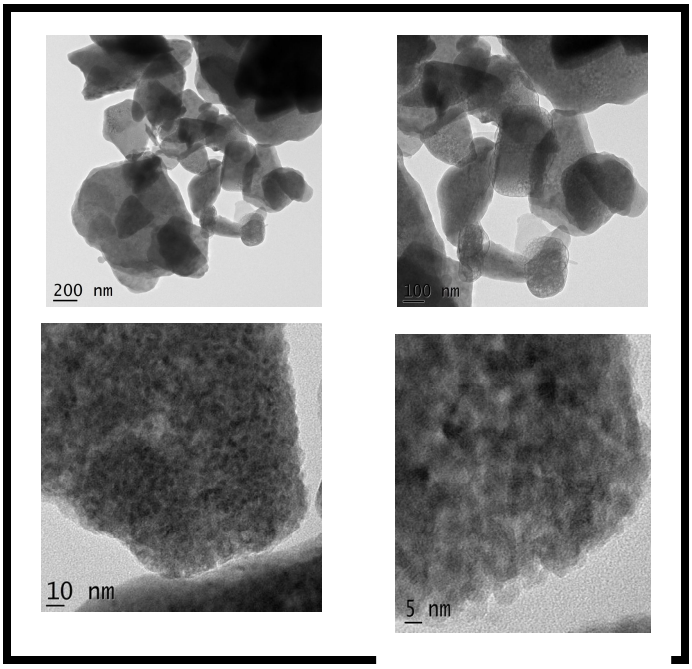

Fig.3-TEM images of 1.0% Zn doped Co ferrite nanoparticles

TEM analysis

Fig. 3 demonstrates the TEM images and SAED example of Zn doped Co-ferrite nanoparticles. For the most part TEM investigation was performed to picture the size, shape and to confirm the nano crystalline nature of the Zn-Co ferrite particles. TEM micrograph displays that the particles are framed in a controlled way with little and uniform estimated grains. Interstingly, it was credited that the sizes of the nanocrystals dictated by TEM were in well correlated with the size acquired from X-ray beam diffractograms.

FTIR Spectroscopy

The FTIR spectra of Co-Zn ferrite samples are shown in Fig. 4. All spectra consist of two main peaks located at about 871cm^{-1} and 1639 cm^{-1}, which confirmed the formation of spinel ferrite structure [33]. The ~ 1409 cm^{-1} peaks is due to vibration mode of tetrahedral sublattice, while ~3432cm^{-1} peak is owing to vibration mode of octahedral sublattice in the spinel structure. Structural and FTIR data of spinel ferrite are utilized for the estimation of elastic moduli and the Debye temperature. The Debye temperature of each sample is measured using the wavenumber of IR bands [34]:

$$\theta_D = \frac{\hbar C v_{av}}{k}$$

Where, $\hbar = h/2\pi$ k is the Boltzmann constant, C is velocity of light (c = 3 × 108 cm/s), and υav is the average wavenumber of bandsIt is observed that the Debye temperature decreases with increasing Zn2+ content and can be associated to the decrease in wavenumber of the peak usually attributed to Me-O bond vibration in the tetrahedral site. The Different elastic moduli for cubic structure are measured used the standard relations discussed elsewhere [34–36]: Figure 4 displays that with increasing Zn content, each elastic moduli increase except B. This behavior of elastic moduli is attributed to the interatomic bonding between various cation within spinel ferrites. The values of Poisson's ratio for each samples remain almost constant, i.e., in the range 0.19–0.27. It has been recorded that a value that lies within the range between−1 and 00.5 implies a good elastic behavior and is in accordance with the theory of isotropic elasticity [34, 36]. This value of the Poisson ratio is in good agreement with Al-substituted $Mn0.5Zn0.5Fe_2O_4$ ferrite [36].

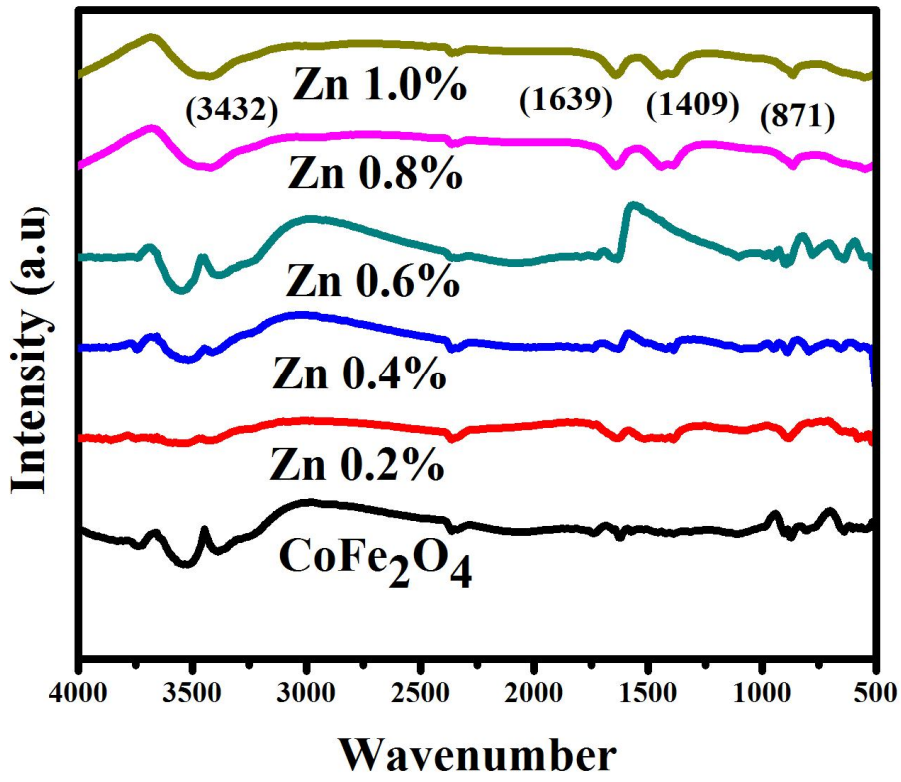

Fig.4- FTIR spectra for $Zn_xCoFe_{2-x}O_4$ with x = 0.0 (a), 0.2 (b), 0.4 (c), 0.6 (d), 0.8 (e) and 1.0 (f)

Optical properties

Fig. 5 shows the UV-visible transmittance spectra of the Zn substituted Co ferrites, the transmittance increases as the doping of Zn. Fig. 5 black colour shows at x = 0, the tranmittance is very low but at x = 1, the absorption is maximum. For the other four diverse concentrations *i.e.* (at x

= 0.2, 0.4, 0.6, 0.8 &1) transmittance is very near to each other but at lower wavelength its value is high. But the common movement for all the six curves displays the same behavior.

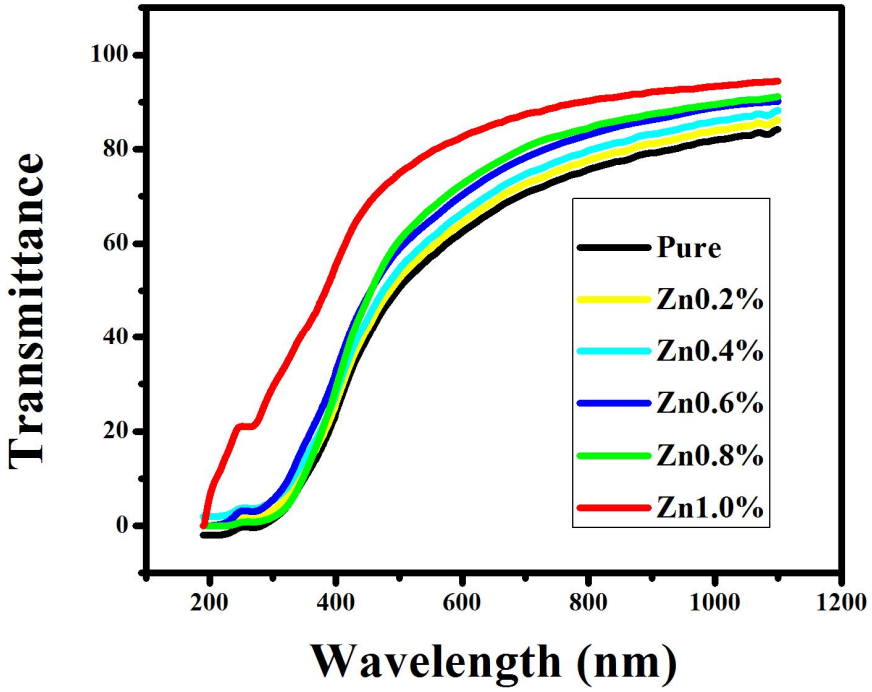

Fig.5- UV Transmittance spectra for $Zn_xCoFe_{2-x}O_4$ with x = 0.0, 0.2, 0.4, 0.6, 0.8 and 1.0%

Raman spectroscopy

Raman spectroscopy system was used to comprehend the arrangement and clarity of prepared Zn doped cobalt ferrite nanoparticles. The Raman spectra of undoped and Zn doped cobalt ferrite nanoparticles are presented in Fig.6. The most exhaustive Raman modes of cobalt ferrite were $3F_{2g}$ (212, 482 and 577 cm^{-1}), one E_g (333 cm^{-1}) and one A_{1g} (702 cm^{-1}) modes [37]. Raman peaks over the region of 565 - 735 cm^{-1} stand for the vibrational modes of octahedral-site and those in the 1119-1364 cm^{-1} area corresponds to the vibrational modes of tetrahedral-site of ferrites [38]. In the present synthesized samples, the vibrational mode with Raman shift observed around at 642 cm^{-1}, which is originated due to the metal-oxide bond in the tetrahedral site [39]. Raman spectra established the absence of any impurity in Al^{3+} doped cobalt ferrite nanoparticles.

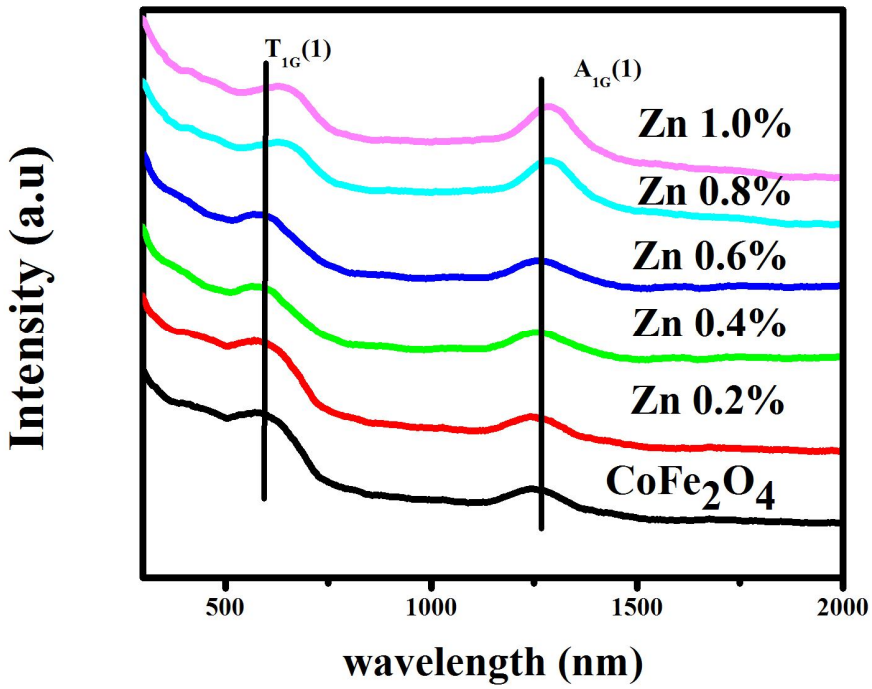

Fig.6- Raman spectra f $Zn_xCoFe_{2-x}O_4$ (0.0-1.0) nanoparticles.

VSM Measurements

$CoFe_2O_4$ displayed a ferromagnetic behavior with a wide hysteresis loop (Fig. 6). Doping with Zn ions reveals also a ferromagnetic behavior while induces important changes in the magnetic properties; the hysteresis loop reduced drastically with Zn content. Ms was found to increase with Zn to reach an optimum value of 114 emu/g for 20% Zn content and then decrease to 82 emu/g for 50% Zn content (Fig. 6). At lower concentrations, Zn ions occupy preferentially tetrahedral A sites of $CoFe_2O_4$ whereas for higher concentration, Zn ions have the tendency to move to octahedral B sites (Fe). It is surprisingly interesting that the substitution of magnetic Co (μB = 3) with a nonmagnetic Zn (μB = 0) shows in a 25% increase in Ms Value. HC is found to reduced with increasing the concentration of Zn. HC decreases drastically by more than 50% with only 10% of Zn, while Mr decreases linearly and slowly with Zn content reaching a reduction of 77% for 50% Zn substitution in comparison with pure $CoFe_2O_4$. It is recorded that at particular range of grain size, HC and Mr become highly sensitive to the changed in grain size [40], which is consistent with the obtainable conclusion. At smaller ranges of crystallite size (D), HC and Mr shows a rapid reduction as D increases, as a slow decrease is noticed as D gets larger. This relation is significant for the Zn-doped $CoFe_2O_4$.

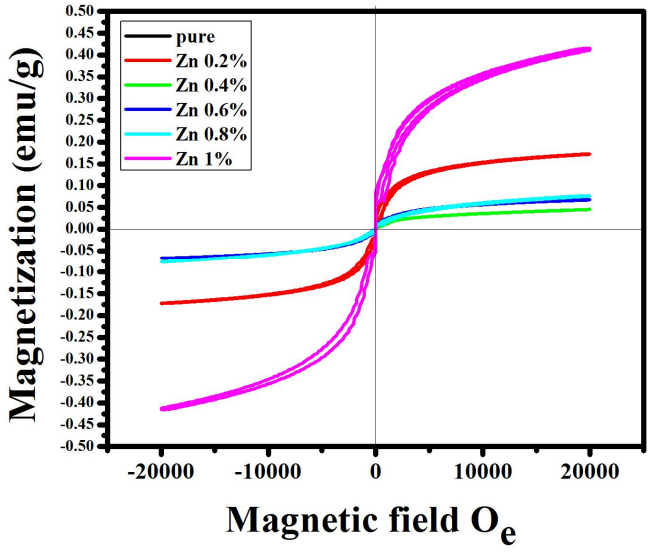

Fig.7- M-H loop of $Zn_xCoFe_{2-x}O_4$ (0.0-1.0) nanoparticles.

Antibacterial Activity

Interestingly, Zn doped is a promising candidate which shows an excellent antibacterial activity against all bacteria. In this present work antibacterial activity of undoped and Zn doped cobalt ferrite against bacterial strains *Escherichia coli, S. Haemolyticus, Aeromonas hydrophila, Cronobacter sakazakii, Aeromonas salmonicida* and *Basillus subtilis* were investigated by the disc diffusion agar method. From the table it is evident that both undoped and Zn doped Cobalt ferrite showed activity towards all pathogens. From the table it is found that zone of inhibition of Zn doped cobalt ferrite is higher than that of the undoped cobalt ferrite which may be due to the reason that the particle size is lower in case of Zn doped cobalt ferrite. This implies that the particle size is one of the key factors to influence the antibacterial activity. Sourav Das et al. 2017 [41] stated the similar results of antibacterial activity against *Escherichia coli* by Solar-Photocatalysis using Fe-doped ZnO. Jones et al. [42] tried to identify the potential antibacterial effect of ZnO nano structure against both Gram-positive (*S.aureus, Bacillus subtilis*) and Gram-negative *(E.coli)* microorganisms. In comparison with these results mentioned above, our results showed better growth of inhibition against both bacteria.

Table 2- Antibacterial activity of pure and Zn doped sample

Zone of inhibition(mm) from pure and Zn doped sample		
strains	**Pure**	**Zn doped**
E.coli (KF 918342)	21.3±0.6	27.6±0.6
S. Haemolyticus	24±0	26.3±0.6
Aeromonas hydrophila	21±1	27±0
Basillus subtilis	20.6±1.1	28.3±0.6
Cronobacter sakazakii	22.3±0.6	25.6±0.6
Aeromonas salmonicida	19.6±1.5	27±1

CONCLUSIONS

Zn-doped $CoFe_2O_4$ NPs have been successfully synthesized using of chemical co-precipitation route. XRD and FTIR proved the formation of single cubic spinel phase. Doping with Zn displayed a considerable effect on structural, spectral, and magnetic properties. The crystallite size and lattice parameter increase gradually while increasing Zn content. This can be associated with ionic radii (Zn is larger than Co) and that Zn favors grain improvment. The line broadening was analyzed by the Scherrer formula, W-H analysis, and the SSP technique. The TEM result was in good agreement with the conclusion of the SSP method. SEM analysis displayed spherical-shaped particles forming agglomerates. The energy gap (Eg) is found to increase for 10% Zn and then remains constant for higher doping level. Magnetic measurements reveal a ferromagnetic behavior while the hysteresis loop tends to reduce with Zn concentration. Ms is found to be sensitive to Zn concentration, while Ms and HC decrease dramatically with increasing the amount of Zn.

REFERENCES

1. Kaviyarasu K, Manikandan E, Paulraj P et al. “One dimensional wellaligned CdO nanocrystal by solvothermal method”. J. Alloys. Comp. 2014; 593:67–70.
2. Kaviyarasu K, Manikandan E, Kennedy J, Jayachandran M. “Quantum confinement and photoluminescence of well-aligned CdO nanofibers by a solvothermal route”. Mater Lett 2014; 120:243–245.
3. Kennedy J, Leveneur J, Williams GVM et al. “Fabrication of surface magnetic nanoclusters using low energy ion implantation and electron beam annealing”. Nanotechnology 2011; 22:115602.

4. Kennedy J, Williams GVM, Murmu PP, Ruck BJ. "Intrinsic magnetic order and inhomogeneous transport in Gd-implanted zinc oxide". Phys. Rev. B 2013; 88:214423.
5. Kaviyarasu K, Manikandan E, Kennedy J, Maaza M. "A comparative study on the morphological features of highly ordered MgO:AgO nanocube arrays prepared via a hydrothermal method". RSC Adv. 2015; 5:82421–82428.
6. Kasinathan K, Kennedy J, Elayaperumal M, Henini M, Malik M. "Photodegradation of organic pollutants RhB dye using UV simulated sunlight on ceria based TiO2 nanomaterials for antibacterial applications". Sci. Rep. 2016; 6:38064–38076.
7. Joshi S, Kumar M, Chhoker S et al. "Effect of Gd^{3+} substitution on structural, magnetic, dielectric and optical properties of nanocrystalline $CoFe_2O_4$". J. Magn. Mag. Mater 2017; 426:252–263
8. Vadivela M, Babua RR, Ramamurthib K, Arivanandhanc M. "CTAB cationic surfactant assisted synthesis of $CoFe_2O_4$ magnetic nanoparticles". Ceram Inter 2016; 42:19320–19328
9. Franco A Jr, Pessoni HV. "Neto FO Enhanced high temperature magnetic properties of ZnO-CoFe2O4 ceramic composite". J Alloys Compd 2016; 680:198–205
10. Huang S, Xu Y, Xie M et al. "Synthesis of magnetic $CoFe_2O_4$/g-C3N4 composite and its enhancement of photocatalytic ability under visible-light". Colloids Surf A 2015; 478:71–80
11. Kaviyarasu K, Geetha N, Kanimozhi K, et al. "In vitro cytotoxicity effect and antibacterial performance of human lung epithelial cells A549 activity of zinc oxide doped TiO2 nanocrystals: investigation of bio-medical application by chemical method". Mat. Sci. Eng: C
12. Jesudoss SK, Vijaya JJ, Kennedy LJ et al. "Studies on the efficient dual performance of Mn1–xNixFe_2O_4 spinel nanoparticles in photodegradation and antibacterial activity". J Photochem Photobiol B.2016; 165:121–132
13. Kaviyarasu K, Ayeshamariam A, Manikandan E et al. "Solution processing of CuSe quantum dots: photocatalytic activity under RhB for UV and visible light solar irradiation". Mat Sci Eng: B. 2016; 210:1–9.
14. Dantas J, Leal E, Mapossa AB et al. "Magnetic nanocatalysts of Ni0.5Zn0. 5Fe_2O_4 doped with Cu and performance evaluation in transesterification reaction for biodiesel production". Fuel 2017; 191:463–471
15. Wang M, Huang Y, Chen X et al. "Synthesis of nitrogen and sulfur co-doped graphene supported hollow $ZnFe_2O_4$ nanosphere composites for application in lithium-ion batteries". J Alloys Compd .2017; 691:407–415
16. Agrawal S, Parveen A, Azam A. "Structural, electrical, and optomagnetic tweaking of Zn doped $CoFe_2$-x$ZnxO_4$-δ nanoparticles". J. Magn. Mag. Mater. 2016; 414:144–152

17. Manikandana A, Vijaya JJ, Kennedy LJ, Bououdina M. "Microwave combustion synthesis, structural, optical and magnetic properties of Zn1−xSrxFe_2O_4 nanoparticles". Ceram Inter. 2013; 39:5909–5917 19.
18. Rathi R, Neogi R. "Structural Electric and magnetic properties of Titanium doped Ni-Cu-Zn Ferrite". Mater Today. 2016; 3:2437–2442
19. Wu X, Yun H, Dongn H. "Enhanced infrared radiation properties of $CoFe_2O_4$ by doping with Y3+ via sol–gel auto-combustion". Ceram Inter. 2014; 40:12883–12889
20. Wu X, Yun H, Dongn H, Geng L. "Enhanced infrared radiation properties of $CoFe_2O_4$ by single Ce^{3+}-doping with energy-efficient preparation". Ceram Inter. 2014; 40:5905–5911.
21. Choodamani C, Nagabhushana GP, Ashoka S et al. "Structural and magnetic studies of Mg(1−x)ZnxFe_2O_4 nanoparticles prepared by a solution combustion method". J. Alloys Compd. 2013; 578:103–109
22. Gabal MA, Al-Juaid AA, Al-Rashed SM, et al. "Synthesis, characterization and electromagnetic properties of Zn-substituted $CoFe_2O_4$ via sucrose assisted combustion route". J. Magn. Mag. Mater. 2016;
23. L. Zhao, H. Yang, X. Zhao, L. Yu, Y. Cui, and S. Feng, "Magnetic properties of $CoFe_2O_4$ ferrite doped with rare earth ion". *Materials Letter*. 2006;**60**, 1–6.
24. . K¨oseo˘glu Y, Baykal A, G¨oz¨uak F, and Kavas H, "Structural and magnetic properties of CoxZn1-xFe_2O_4 nanocrystals synthesized by microwave method". *Polyhedron*. 2009;**28**, 2887–2892.
25. Buchanan R. C. *Ceramic Materials for Electronics.* USA: Marcel Dekker, 2004.
26. Goldman A, *Modern Ferrite Technology*. USA: Pittsburgh, 2006.
27. Haertling G. H, Ferroelectric ceramics: history and technology. *J. Am. Ceram Soc*. 1999; **82**, 797–818
28. Tetiana Tatarchuk et.al., Structural, Optical, and Magnetic Properties of Zn-Doped $CoFe_2O_4$ Nanoparticles, Tatarchuk et al. Nanoscale Research Letters 2017.
29. . Kumar L, Kumar P, Narayan A, Kar M. "Rietveld analysis of XRD patterns of different sizes of nanocrystalline cobalt ferrite". Int. Nano Lett. 2013; 3:8.
30. Yu¨ksel Koseo ¨ glu˘ a,n , Mousa Ibrahim Oleiwi Oleiwia , Resul Yilginb , Abdullah N. Koc-bay. "Effect of chromium addition on the structural, morphological and magnetic properties of nano-crystalline cobalt ferrite system", Ceramics International 38 2012; 6671–6676
31. Dipali S. Nikam, Swati V. Jadhav, Vishwajeet M. Khot, R.A. Bohara, Chang K. Hong, Sawanta S. Malib, S.H. Pawar, RSC Adv. 5 2015; 2338

32. Panda R.K, Muduli R, Jayarao G, Sanyal D, Behera D. "Effect of Cr^{3+} substitution on electric and magnetic properties of cobalt ferrite nanoparticles", Journal of Alloys and Compounds 2016; 669 :19-28
33. Tatarchuk TR, Bououdina M, Paliychuk ND et al. "Structural characterization and anti structure modeling of cobalt-substituted zinc ferrites". J Alloys Compd. 2017 694:777–791.
34. Patange SM, Shirsath SE, Jadhav SP et al. "Elastic properties of nanocrystalline aluminum substituted nickel ferrites prepared by coprecipitation method". J. Mol. Struct. 2013; 1038:40–44.
35. Modi KB, Raval PY, Shah SJ et al. "Raman and Mossbauer spectroscopy and X-ray diffractometry studies on quenched Copper–Ferri–Aluminates". Inorg. Chem. 2015; 54(4):1543–1555.
36. Mohamed MB, Wahba AM. "Structural, magnetic, and elastic properties of nanocrystalline Al-substituted $Mn0.5Zn0.5Fe_2O_4$ ferrite". Ceram Inter. 2014; 40:11773–11780,
37. White W, DeAngelis B. "Interpretation of the vibrational spectra of spinels, Spectrochimica Acta Part A: Molecular Spectroscopy", 1967; 23: 985-995.
38. Wang Z, Lazor P, Saxena S, H.S.C. O'Neill, "High pressure Raman spectroscopy of ferrite $MgFe_2O_4$, Materials Research Bulletin". 2002; 37: 1589-1602.
39. Chandramohan P, Srinivasan M, Velmurugan S, Narasimhan S. "Cation distribution and particle size effect on Raman spectrum of $CoFe_2O_4$", Journal of Solid State Chemistry. 2011; 184: 89-96.
40. Vollath D. Nanomaterials: "An introduction to synthesis, properties and applications". WILEY-VCH Verlag GmbH & Co.KGaA, Germany.2008
41. Das S, Sinha S, Das B, Jayabalan R, Suar M, Mishra A, Tripathy S. K. "Disinfection of Multidrug Resistant *Escherichia coli* by Solar-Photocatalysis using Fe-doped ZnO Nanoparticles". *Sci. Rep.* 2017;7: 104.
42. Jones N, Ray B, Ranjit K. T, Manna A. C. "Antibacterial activity of ZnO nanoparticle suspensions on a broad spectrum of microorganisms". *FEMS Microbiol. Lett.* 2008; 279: 71-76.